DOI 10.1007/s10946-015-9522-z
*Journal of Russian Laser Research, Volume 36, Number 5, September, 2015*

# TESTING ENTROPIC INEQUALITIES FOR SUPERCONDUCTING QUDITS

**Evgenii Glushkov,[1,2]* Anastasiia Glushkova,[1] and Vladimir I. Man'ko[3,4]**

[1] *Moscow Institute of Physics and Technology (State University)*
*Institutskií per. 9, Dolgoprudnyí, Moscow Region 141700, Russia*

[2] *National University of Science and Technology "MISiS"*
*Leninskii Prospect 4, Moscow 119991, Russia*

[3] *Lebedev Physical Institute, Russian Academy of Sciences*
*Leninskii Prospect 53, Moscow 119991, Russia*

[4] *Physics Department, Tomsk State University*
*Lenin Avenue 36, Tomsk 634050, Russia*

*Corresponding author e-mail: eugene.glushkov @ gmail.com

**Abstract**

We verify the new entropic and information inequalities for noncomposite systems using an experimental 5×5 density matrix of the qudit state measured by the tomographic method in a multilevel superconducting circuit. These inequalities are well known for bipartite and tripartite systems but have never been tested for superconducting qudits. Entropic inequalities can also be used to evaluate the accuracy of experimental data and the value of mutual information deduced from them and characterize correlations between different degrees of freedom in a noncomposite system.

**Keywords:** entropic inequalities, noncomposite systems, superconducting qubits.

## 1. Introduction

During the last few decades, tremendous progress has been made in experimental control over quantum systems. In particular, experiments with superconducting circuits based on Josephson junction devices [1, 2] have been rapidly developing recently [3]. Specifically, the spectroscopic [4, 5] and time-domain [6] properties of such systems were studied both theoretically and experimentally. With the improvement of coherence time of superconducting qubits, it became possible to obtain the density matrices of such systems, using the quantum-state tomography [7] as well as the Wigner tomography [8].

Along with the development of quantum circuits, the properties of composite quantum systems, i.e., the systems containing subsystems, have been extensively studied, which resulted in numerous practical applications. These systems were also described in terms of classical information theory [9] in the quantum domain [10], and their information and entropic characteristics were investigated, including the von Neumann entropy and quantum mutual information, discord-related measures, entropic inequalities, contextuality, causality, and the subadditivity and strong subadditivity conditions.

In contrast, the idea of using noncomposite quantum systems for quantum technologies was suggested [11–13], and quantum correlations in such systems have been analyzed only recently [14, 15]. The

Manuscript submitted by the authors in English on August 19, 2015.


1071-2836/15/3605-0448 

latter opened a way of mapping information and entropic measures for composite quantum systems on the noncomposite quantum systems [14–19].

In this work, we aim to verify the entropic and information inequalities using an experimental 5×5 density matrix of the qudit state ($j = 2$) obtained by the direct Wigner tomography in a superconducting circuit [8, 20, 21]. The inequalities were obtained employing the approach [14–18] to find analogs of the subadditivity and strong subadditivity conditions, well known for bipartite and tripartite systems, for a single qudit state.

## 2. Superconducting Circuits

Superconducting circuits with Josephson junctions are macroscopic quantum objects which can be of several micrometers wide while still preserving quantum properties. This happens because they are artificially isolated from the environment, which leaves them with a single degree of freedom. The intrinsic parameters of these circuits can be engineered as desired and adjusted with an external parameter (for example, a magnetic field); so they are often called artificial atoms.

### 2.1. Josephson Junction

The Josephson junction in superconducting circuits serves as a nondissipative nonlinear element. It consists of two superconductors separated by a thin insulating layer, through which Cooper pairs can coherently tunnel. This system was described by Brian Josephson [22], who showed that the supercurrent across the junction depends on the phase difference between the superconductors

$$I = I_c \sin(\phi_2 - \phi_1) = I_c \sin\phi, \tag{1}$$

where $I_c$ stands for the maximum nondissipative current flowing through the junction, i.e., the critical current. Josephson also showed that, when the voltage is applied across the junction, the phase difference changes in time, which leads to the oscillations of the critical current with the angular frequency $\omega$:

$$\hbar\dot{\phi} = \hbar\omega = 2\,\mathrm{eV}. \tag{2}$$

Substituting this phase difference into the time derivative of Eq. (1) and comparing it with the Faraday law, we obtain the Josephson inductance

$$L_J(\phi) = \frac{\hbar}{2eI_c\cos\phi} = \frac{\Phi_0}{2\pi(I_c^2 - I^2)^{1/2}}\,. \tag{3}$$

As the Josephson junction has some intrinsic capacity $C$, it behaves as a nonlinear oscillator with angular frequency $\omega_p$

$$\omega_p(I) = \frac{1}{\sqrt{L_J C}} = \frac{(2\pi I_c/\Phi_0 C)^{1/2}}{(1 - I^2/I_c^2)^{1/4}}\,. \tag{4}$$

The total current flow trough the junction can be written as $J = I_c\sin\phi + (V/R) + C\dot{V}$. Substituting $\dot{V} = (\hbar/2e)\ddot{\phi}$ from Eq. (2), we arrive at

$$J = I_c\sin\phi + \frac{1}{R}\frac{\Phi_0}{2\pi}\dot{\phi} + C\frac{\Phi_0}{2\pi}\ddot{\phi}, \tag{5}$$

which is equivalent to the equation of motion of a particle moving in a tilted washboard potential

$$m\ddot{\phi} + m\frac{1}{\mathrm{RC}}\dot{\phi} + \frac{\partial U(\phi)}{\partial \phi} = 0, \tag{6}$$

where $U = -\dfrac{I_c\Phi_0}{2\pi}\left(\dfrac{I}{I_c}\phi + \cos\phi\right)$; see Fig. 2.1.

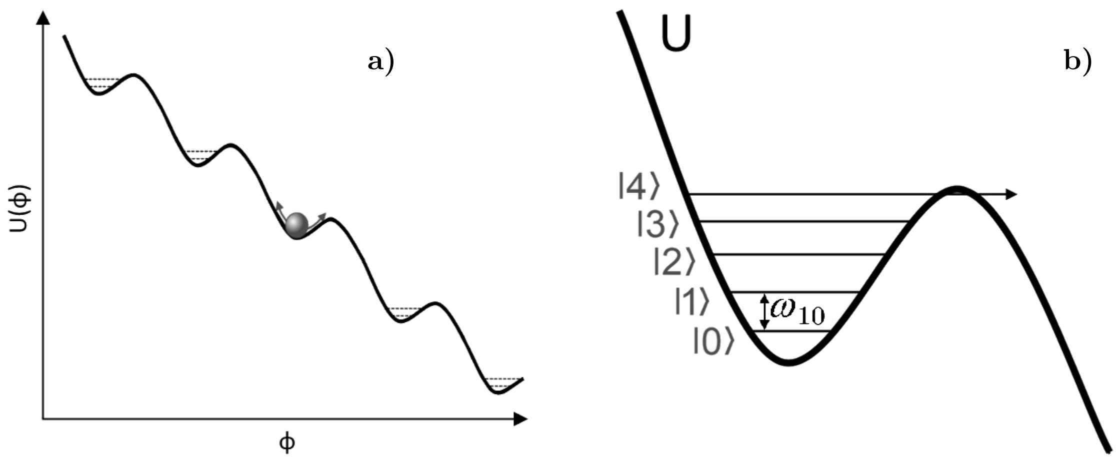


**Fig. 1.** Tilted washboard potential (a) and quantized energy levels inside one of the potential wells (b).

## 2.2. Superconducting Qudit

A closer look at one of the wells in the tilted washboard potential in Fig. 2 b with the quantized energy levels gives us a perfectly suitable d-level system (qudit). Varying the potential by an external magnetic field, we can achieve the desired number of energy levels in the well. The physical implementation of this system is called the Josephson phase circuit [23, 24]; it is shown in Fig. 2.

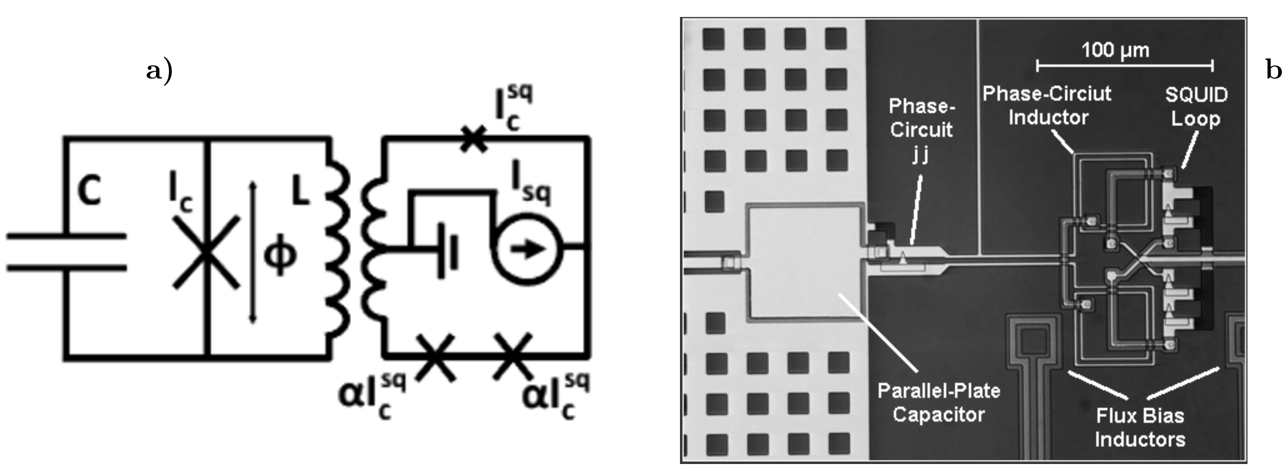


**Fig. 2.** The Josephson phase circuit (JPC) with an on-chip SQUID. The schematic diagram of the circuit (a). The left-hand side corresponds to the JPC, and the right-hand side shows the on-chip SQUID, which is used for the readout. The micrograph of the fabricated sample (b). [Images adopted from [20].]

The quantum state of the Josephson phase circuit is controlled through pulses of the bias current. The measurement of the state employs the escape from the potential well via tunneling. For example, to measure the occupation probability of the state $|1\rangle$, one can pump microwaves at frequency $\omega_{41}$, which will induce a $|1\rangle \to |4\rangle$ transition. Then the state will rapidly tunnel due to the large tunneling rate $\Gamma_4$. When the tunneling occurs, a voltage appears across the junction, which can be measured directly by an on-chip SQUID.

In this paper, we employ the results obtained in the experiment by Shalibo et al. [8, 20, 21], where the Wigner distribution of the Josephson phase circuit was directly measured using simple tomography pulses.

## 3. Entropic Inequalities

Quantum states are described by the density matrices of operators $\hat{\rho}$ with the following properties:

$$\mathrm{Tr}(\hat{\rho}) = 1, \qquad \hat{\rho} = \hat{\rho}^\dagger, \qquad \hat{\rho} \geq 0. \tag{7}$$

We consider a 5×5 density matrix $\rho = \begin{pmatrix} \rho_{11} & \rho_{12} & \rho_{13} & \rho_{14} & \rho_{15} \\ \rho_{21} & \rho_{22} & \rho_{23} & \rho_{24} & \rho_{25} \\ \rho_{31} & \rho_{32} & \rho_{33} & \rho_{34} & \rho_{35} \\ \rho_{41} & \rho_{42} & \rho_{43} & \rho_{44} & \rho_{45} \\ \rho_{51} & \rho_{52} & \rho_{53} & \rho_{54} & \rho_{55} \end{pmatrix}$ for a qudit with $j = 2$. We can be rewrite this matrix as a 6×6 matrix $\rho = \begin{pmatrix} \rho_{11} & \rho_{12} & \rho_{13} & \rho_{14} & \rho_{15} & 0 \\ \rho_{21} & \rho_{22} & \rho_{23} & \rho_{24} & \rho_{25} & 0 \\ \rho_{31} & \rho_{32} & \rho_{33} & \rho_{34} & \rho_{35} & 0 \\ \rho_{41} & \rho_{42} & \rho_{43} & \rho_{44} & \rho_{45} & 0 \\ \rho_{51} & \rho_{52} & \rho_{53} & \rho_{54} & \rho_{55} & 0 \\ 0 & 0 & 0 & 0 & 0 & 0 \end{pmatrix}$ by adding one more zero row and zero column.

Looking at this system, one can realize that it can be viewed as a tensor product of two subsystems: a qubit and a qutrit. So, using an invertible mapping of indices

$$1 \leftrightarrow -1 \;\; -1/2; \quad 2 \leftrightarrow -1 \;\; 1/2; \quad 3 \leftrightarrow 0 \;\; -1/2; \quad 4 \leftrightarrow 0 \;\; 1/2; \quad 5 \leftrightarrow 1 \;\; -1/2; \quad 6 \leftrightarrow 1 \;\; 1/2,$$

we obtain the density matrix, which describes the bipartite qubit–qutrit state. The density matrices of the subsystems are usually derived by taking the partial trace over the corresponding indices. We propose a simplified approach by dividing the density matrix into blocks (see, for example, [25]) with fewer dimensions, namely,

$$\rho = \left(\begin{array}{ccc|ccc} \rho_{11} & \rho_{12} & \rho_{13} & \rho_{14} & \rho_{15} & 0 \\ \rho_{21} & \rho_{22} & \rho_{23} & \rho_{24} & \rho_{25} & 0 \\ \rho_{31} & \rho_{32} & \rho_{33} & \rho_{34} & \rho_{35} & 0 \\ \hline \rho_{41} & \rho_{42} & \rho_{43} & \rho_{44} & \rho_{45} & 0 \\ \rho_{51} & \rho_{52} & \rho_{53} & \rho_{54} & \rho_{55} & 0 \\ 0 & 0 & 0 & 0 & 0 & 0 \end{array}\right) = \begin{pmatrix} R_{11} & R_{12} \\ R_{21} & R_{22} \end{pmatrix}. \tag{8}$$

Then the density matrices of the subsystems are

$$\rho_1 = \begin{pmatrix} \mathrm{Tr}\, R_{11} & \mathrm{Tr}\, R_{12} \\ \mathrm{Tr}\, R_{21} & \mathrm{Tr}\, R_{22} \end{pmatrix} = \begin{pmatrix} \rho_{11}+\rho_{22}+\rho_{33} & \rho_{14}+\rho_{25} \\ \rho_{41}+\rho_{52} & \rho_{44}+\rho_{55} \end{pmatrix} \tag{9}$$

and

$$\rho_2 = (R_{11}+R_{22}) = \begin{pmatrix} \rho_{11}+\rho_{44} & \rho_{12}+\rho_{45} & \rho_{13} \\ \rho_{21}+\rho_{54} & \rho_{22}+\rho_{55} & \rho_{23} \\ \rho_{31} & \rho_{32} & \rho_{33} \end{pmatrix}. \tag{10}$$

Now we can check the correlations in the system. One of the most important correlation characteristics is entropy. In this work, we deal with the von Neumann entropy [26]

$$S_N = -\,\mathrm{Tr}\,\rho \ln \rho. \tag{11}$$

For the von Neumann entropy of the bipartite system, one can write the subadditivity condition $S_\rho \leq S_{\rho_1} + S_{\rho_2}$ as follows:

$$-\,\mathrm{Tr}\,\rho\ln\rho \leq -\,\mathrm{Tr}\,\rho_1\ln\rho_1 - \mathrm{Tr}\,\rho_2\ln\rho_2 \tag{12}$$

and introduce the mutual information

$$I_{bp1} = S_{\rho_1} + S_{\rho_2} - S_\rho. \tag{13}$$

Now we can repeat this process for the other partition of the 6×6 density matrix:

$$\rho = \left(\begin{array}{cc|cc|cc} \rho_{11} & \rho_{12} & \rho_{13} & \rho_{14} & \rho_{15} & 0 \\ \rho_{21} & \rho_{22} & \rho_{23} & \rho_{24} & \rho_{25} & 0 \\ \hline \rho_{31} & \rho_{32} & \rho_{33} & \rho_{34} & \rho_{35} & 0 \\ \rho_{41} & \rho_{42} & \rho_{43} & \rho_{44} & \rho_{45} & 0 \\ \hline \rho_{51} & \rho_{52} & \rho_{53} & \rho_{54} & \rho_{55} & 0 \\ 0 & 0 & 0 & 0 & 0 & 0 \end{array}\right) = \begin{pmatrix} r_{11} & r_{12} & r_{13} \\ r_{21} & r_{22} & r_{23} \\ r_{31} & r_{32} & r_{33} \end{pmatrix} \tag{14}$$

and obtain the density matrices of the subsystems

$$\tilde\rho_1 = \begin{pmatrix} \mathrm{Tr}\, r_{11} & \mathrm{Tr}\, r_{12} & \mathrm{Tr}\, r_{13} \\ \mathrm{Tr}\, r_{21} & \mathrm{Tr}\, r_{22} & \mathrm{Tr}\, r_{23} \\ \mathrm{Tr}\, r_{31} & \mathrm{Tr}\, r_{32} & \mathrm{Tr}\, r_{33} \end{pmatrix} = \begin{pmatrix} \rho_{11}+\rho_{22} & \rho_{13}+\rho_{24} & \rho_{15} \\ \rho_{31}+\rho_{42} & \rho_{33}+\rho_{44} & \rho_{35} \\ \rho_{51} & \rho_{53} & \rho_{55} \end{pmatrix} \tag{15}$$

and

$$\tilde\rho_2 = (r_{11}+r_{22}+r_{33}) = \begin{pmatrix} \rho_{11}+\rho_{33}+\rho_{55} & \rho_{12}+\rho_{34} \\ \rho_{21}+\rho_{43} & \rho_{22}+\rho_{44} \end{pmatrix}. \tag{16}$$

So the subadditivity condition $S_\rho \leq S_{\tilde\rho_1} + S_{\tilde\rho_2}$ reads

$$-\,\mathrm{Tr}\,\rho\ln\rho \leq -\,\mathrm{Tr}\,\tilde\rho_1\ln\tilde\rho_1 - \mathrm{Tr}\,\tilde\rho_2\ln\tilde\rho_2, \tag{17}$$

and the mutual information is

$$I_{bp2} = S_{\tilde{\rho}_1} + S_{\tilde{\rho}_2} - S_{\rho}. \tag{18}$$

Next, we add two more zero rows and columns to this matrix, in order to obtain an 8×8 matrix. The system described by this density matrix can be divided into three subsystems (represented by 2×2 matrices) using the following mapping of indices:

$$\begin{array}{ll} 1 \leftrightarrow -1/2\ \ -1/2\ \ -1/2; & 2 \leftrightarrow -1/2\ \ -1/2\ 1/2; \\ 3 \leftrightarrow -1/2\ 1/2\ \ -1/2; & 4 \leftrightarrow -1/2\ 1/2\ 1/2; \\ 5 \leftrightarrow 1/2\ \ -1/2\ \ -1/2; & 6 \leftrightarrow 1/2\ \ -1/2\ 1/2; \\ 7 \leftrightarrow 1/2\ 1/2\ \ -1/2; & 8 \leftrightarrow 1/2\ 1/2\ 1/2. \end{array}$$

Here, we use the same approach of dividing the matrix into blocks to calculate the partial traces and get the matrices for the subsystems

$$\rho = \left(\begin{array}{cccc|cccc} 0 & 0 & 0 & 0 & 0 & 0 & 0 & 0 \\ 0 & \rho_{11} & \rho_{12} & \rho_{13} & 0 & \rho_{14} & \rho_{15} & 0 \\ 0 & \rho_{21} & \rho_{22} & \rho_{23} & 0 & \rho_{24} & \rho_{25} & 0 \\ 0 & \rho_{31} & \rho_{32} & \rho_{33} & 0 & \rho_{34} & \rho_{35} & 0 \\ \hline 0 & 0 & 0 & 0 & 0 & 0 & 0 & 0 \\ 0 & \rho_{41} & \rho_{42} & \rho_{43} & 0 & \rho_{44} & \rho_{45} & 0 \\ 0 & \rho_{51} & \rho_{52} & \rho_{53} & 0 & \rho_{54} & \rho_{55} & 0 \\ 0 & 0 & 0 & 0 & 0 & 0 & 0 & 0 \end{array}\right) = \left(\begin{array}{cc|cc|cc|cc} 0 & 0 & 0 & 0 & 0 & 0 & 0 & 0 \\ 0 & \rho_{11} & \rho_{12} & \rho_{13} & 0 & \rho_{14} & \rho_{15} & 0 \\ \hline 0 & \rho_{21} & \rho_{22} & \rho_{23} & 0 & \rho_{24} & \rho_{25} & 0 \\ 0 & \rho_{31} & \rho_{32} & \rho_{33} & 0 & \rho_{34} & \rho_{35} & 0 \\ \hline 0 & 0 & 0 & 0 & 0 & 0 & 0 & 0 \\ 0 & \rho_{41} & \rho_{42} & \rho_{43} & 0 & \rho_{44} & \rho_{45} & 0 \\ \hline 0 & \rho_{51} & \rho_{52} & \rho_{53} & 0 & \rho_{54} & \rho_{55} & 0 \\ 0 & 0 & 0 & 0 & 0 & 0 & 0 & 0 \end{array}\right). \tag{19}$$

The density matrices that we are using hereinafter are the matrix of the second subsystem $R_2$ and two joint matrices of the qubit–qubit subsystems $\rho_{12}$ and $\rho_{23}$

$$R_2 = \begin{pmatrix} \rho_{11}+\rho_{14}+\rho_{41}+\rho_{44} & \rho_{13}+\rho_{43} \\ \rho_{31}+\rho_{34} & \rho_{22}+\rho_{33}+\rho_{25}+\rho_{52}+\rho_{55} \end{pmatrix}, \quad \rho_{12} = \begin{pmatrix} \rho_{11} & \rho_{13} & \rho_{14} & 0 \\ \rho_{31} & \rho_{22}+\rho_{33} & \rho_{34} & \rho_{25} \\ \rho_{41} & \rho_{43} & \rho_{44} & 0 \\ 0 & \rho_{52} & 0 & \rho_{55} \end{pmatrix}, \tag{20}$$

$$\rho_{23} = \begin{pmatrix} 0 & 0 & 0 & 0 \\ 0 & \rho_{11}+\rho_{14}+\rho_{41}+\rho_{44} & \rho_{12}+\rho_{15}+\rho_{42}+\rho_{45} & \rho_{13}+\rho_{43} \\ 0 & \rho_{21}+\rho_{24}+\rho_{51}+\rho_{54} & \rho_{22}+\rho_{25}+\rho_{52}+\rho_{55} & \rho_{23}+\rho_{53} \\ 0 & \rho_{31}+\rho_{34} & \rho_{32}+\rho_{35} & \rho_{33} \end{pmatrix}. \tag{21}$$

For such a kind of the tripartite system, one can write the strong subadditivity condition [27]

$$S_{\rho} + S_{R_2} \leq S_{\rho_{12}} + S_{\rho_{23}}$$

as follows:

$$-\operatorname{Tr}\rho\ln\rho - \operatorname{Tr}R_2\ln R_2 \leq -\operatorname{Tr}\rho_{12}\ln\rho_{12} - \operatorname{Tr}\rho_{23}\ln\rho_{23}. \tag{22}$$

## 4. Verifying the Experimental Data

In this section, we calculate the density matrices of the subsystems from the experimentally obtained 5×5 density matrix. This density matrix corresponds to the qudit described in Sec 2.2 and measured in [8, 20, 21].

The density matrices in Eqs. (9) and (10) read

$$\rho_1=\begin{pmatrix} 0.985 & 8.3\cdot10^{-5}-2.7\cdot10^{-4}\,\mathrm{i}\\ 8.3\cdot10^{-5}+2.7\cdot10^{-4}\,\mathrm{i} & 0.006\end{pmatrix},\quad \rho_2=\begin{pmatrix} 0.96 & 8.8\cdot10^{-4}-0.003\,\mathrm{i} & 0.008-0.018\,\mathrm{i}\\ 8.8\cdot10^{-4}+0.003\,\mathrm{i} & 0.004 & -7.6\cdot10^{-4}-2.9\cdot10^{-4}\,\mathrm{i}\\ 0.008+0.018\,\mathrm{i} & -7.6\cdot10^{-4}+2.9\cdot10^{-4}\,\mathrm{i} & 0.026\end{pmatrix}.$$

The density matrices in Eqs. (15) and (16) are

$$\tilde\rho_1=\begin{pmatrix} 0.96 & 0.008-0.018\,\mathrm{i} & -0.006-8.6\cdot10^{-4}\,\mathrm{i}\\ 0.008+0.018\,\mathrm{i} & 0.028 & 0.005-0.007\,\mathrm{i}\\ -0.006+8.6\cdot10^{-4}\,\mathrm{i} & 0.005+0.007\,\mathrm{i} & 0.004\end{pmatrix},\qquad \tilde\rho_2=\begin{pmatrix} 0.99 & 0.005-0.002\,\mathrm{i}\\ 0.005+0.002\,\mathrm{i} & 0.002\end{pmatrix}.$$

Using these matrices, we can calculate the corresponding entropies and mutual information and test the subadditivity condition for different partitions in Eqs. (12) and (17). Moreover, we can also change the position of the zero row and zero column in Eqs. (8) and (14) to see how these entities will be changed. The results of these calculations are given in Table 1 and shown in Fig. 5.

**Table 1.** Calculated Entropies and Mutual Information.

| Zero-row position | $S_\rho$ | $S_{bp1}$ | $S_{bp2}$ | $I_{bp1}$ | $I_{bp2}$ |
|---|---|---|---|---|---|
| $(1;1)$ | 0.1583 | 0.300 | 0.180 | 0.1418 | 0.0224 |
| $(2;2)$ | 0.1583 | 0.1965 | 0.3040 | 0.0383 | 0.1457 |
| $(3;3)$ | 0.1583 | 0.1968 | 0.3042 | 0.0386 | 0.1459 |
| $(4;4)$ | 0.1583 | 0.2001 | 0.1987 | 0.0418 | 0.0404 |
| $(5;5)$ | 0.1583 | 0.1873 | 0.2059 | 0.0291 | 0.0477 |
| $(6;6)$ | 0.1583 | 0.1996 | 0.1768 | 0.0413 | 0.0185 |

Finally, we calculate the density matrices for the tripartite system, Eqs. (20) and (21); they read

$$\rho_{12}=\begin{pmatrix} 0.959 & 0.008-0.018\,\mathrm{i} & 0.0002-0.0004\,\mathrm{i} & 0\\ 0.008+0.018\,\mathrm{i} & 0.026 & 0.003+0.0013\,\mathrm{i} & -0.0001+0.0002\,\mathrm{i}\\ 0.0002+0.0004\,\mathrm{i} & 0.003-0.0013\,\mathrm{i} & 0.0018 & 0\\ 0 & -0.0001-0.0002\,\mathrm{i} & 0 & 0.004\end{pmatrix},$$

$$\rho_{23}=\begin{pmatrix} 0 & 0 & 0 & 0\\ 0 & 0.961\,\mathrm{i} & -0.005-0.004\,\mathrm{i} & 0.012-0.019\,\mathrm{i}\\ 0 & -0.005+0.004\,\mathrm{i} & 0.004 & 0.004+0.0064\,\mathrm{i}\\ 0 & 0.012+0.019\,\mathrm{i} & 0.004-0.0064\,\mathrm{i} & 0.026\end{pmatrix},$$

$$R_2=\begin{pmatrix} 0.961 & 0.012-0.019\,\mathrm{i}\\ 0.012+0.019\,\mathrm{i} & 0.030\end{pmatrix}.$$

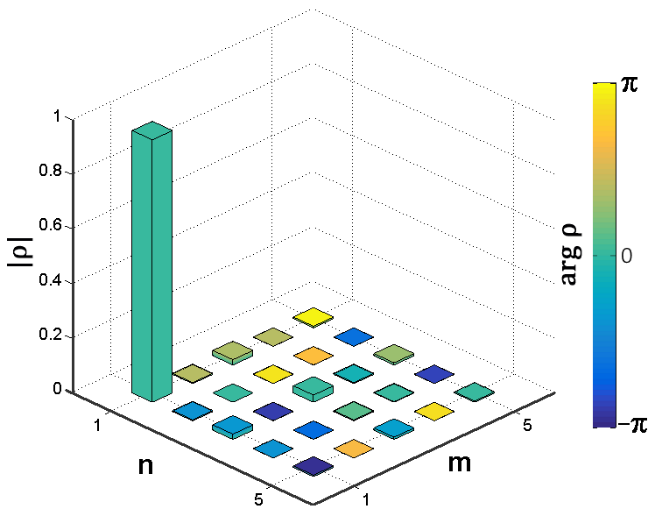


**Fig. 3.** Experimentally obtained density matrix of a superconducting qudit [8, 20, 21].

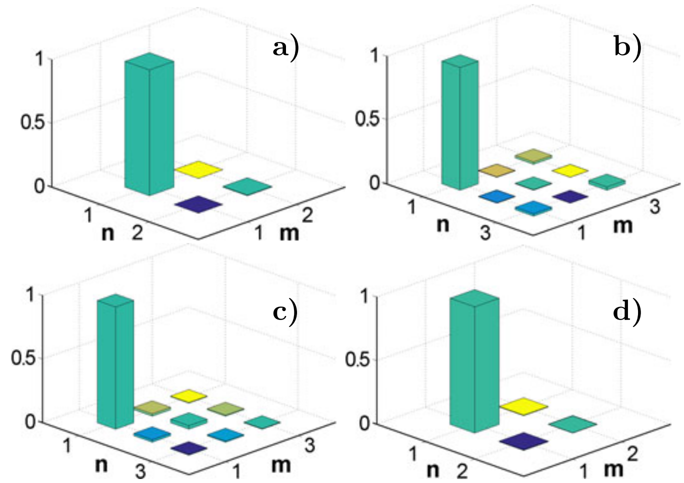


**Fig. 4.** Calculated density matrices for the bipartite system with the first partition $\rho_1$ (a) and $\rho_2$ (b) given by Eqs. (9) and (10) and the second partition $\tilde{\rho}_1$ (c) and $\tilde{\rho}_2$ (d) given by Eqs. (15) and (16).

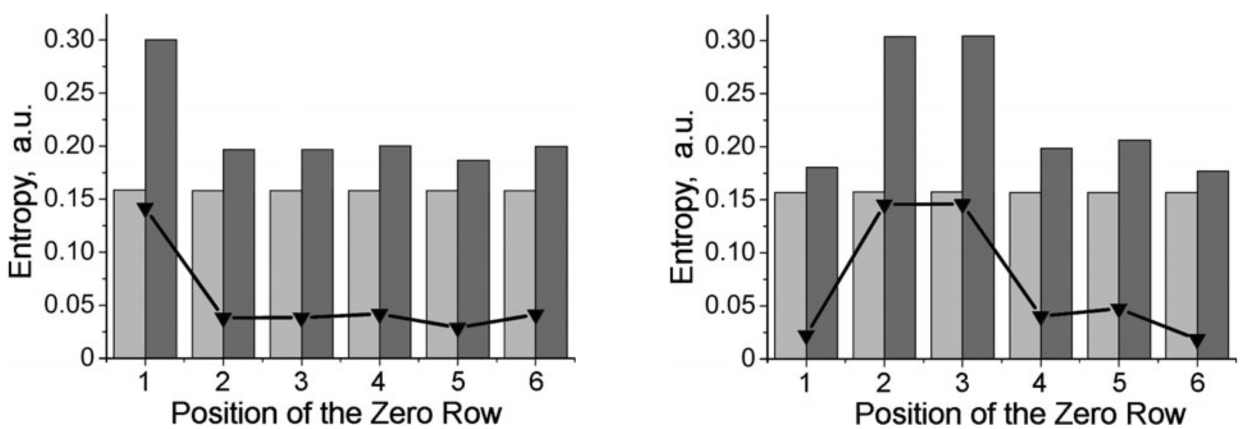


**Fig. 5.** The entropies and mutual information from Table 1 versus the position of the zero row for the qubit–qutrit partition. Here, the first partition on the left and the second partition on the right. Left-side entropy is shown in light gray, right-side entropy is shown in dark gray, and mutual information by the curve.

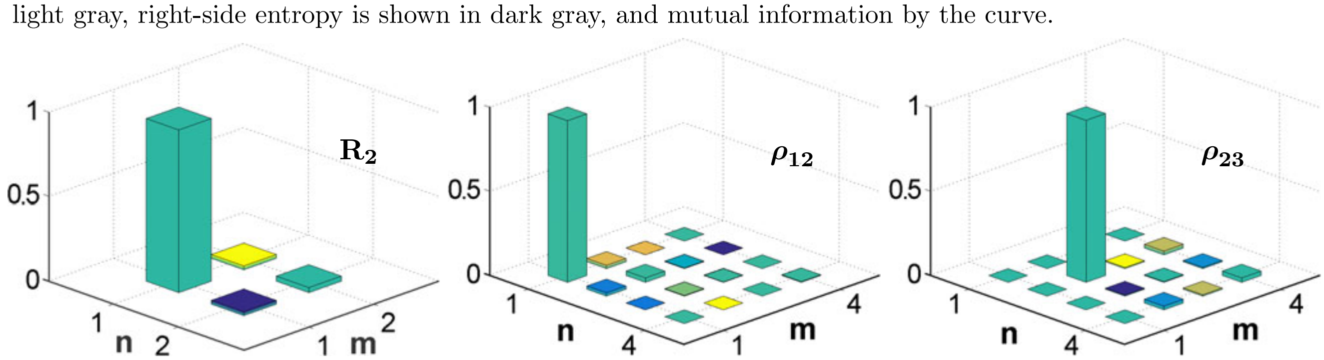


**Fig. 6.** Calculated density matrices of the subsystems for the tripartite system.

The density matrices of the subsystems for the tripartite system calculated in view of the experimental data are shown in Fig. 6.

After calculations, the strong subadditivity condition (22) reads: $0.2997 \leq 0.3142$; so the mutual information is $I = S_{\rho_{12}} + S_{\rho_{23}} - S_\rho - S_{R_2} = 0.3142 - 0.2997 = 0.0147$.

## 5. Conclusions

We checked that the experimentally measured density matrix of a superconducting qudit [8] satisfies the new entropic inequalities for noncomposite systems, given by Eqs. (12), (17), and (22). These inequalities can be further used to evaluate the accuracy of the experimental data. Moreover, the value of mutual information deduced from the entropic inequalities may characterize correlations between different degrees of freedom in a noncomposite system. There also exist other inequalities for the von Neumann entropy and $q$-entropy, which we will check in future publications.

## Acknowledgments

The support by the Ministry for Education and Science of the Russian Federation within the framework of the Increased Competitiveness Program of the National University of Science and Technology MISIS under Contract No. K2-2014-025 is gratefully acknowledged. The authors thank Drs. E. Kiktenko and I. Khrapach for stimulating discussions. V.I.M. was partially supported by the Tomsk State University Competitiveness Improvement Program.

## References

1. V. V. Dodonov, V. I. Man'ko, and O. V. Man'ko, *J. Sov. Laser Res.*, **10**, 413 (1989).
2. T. Fujii, S. Matsuo, N. Hatakenaka, et al., *Phys. Rev. B*, **84**, 174521 (2011).
3. J. Clarke and F. K. Wilhelm, *Nature*, **453**, 1031 (2008).
4. Y. Nakamura, C. Chen, and J. Tsai, *Phys. Rev. Lett.*, **79**, 2328 (1997).
5. A. Averkin, A. Karpov, K. Shulga, et al., *Rev. Sci. Instrum.*, **85**, 104702 (2014).
6. I. Chiorescu, Y. Nakamura, C.-M. Harmans, and J. Mooij, *Science*, **299**, 1869 (2003).
7. M. Steffen, M. Ansmann, R. McDermott, et al., *Phys. Rev. Lett.*, **97**, 050502 (2006).
8. Y. Shalibo, R. Resh, O. Fogel, et al., *Phys. Rev. Lett.*, **110**, 100404 (2013).
9. C.-E. Shannon, *Bell Syst. Tech. J.*, **27**, 379 (1948).
10. A. S. Holevo, *Quantum Systems, Channels, Information: a Mathematical Introduction*, Walter de Gruyter (2012), Vol. 16.
11. A. Fedorov, E. Kiktenko, O. V. Man'ko, and V. I. Man'ko, arXiv:1411.0157 (2014).
12. E. Kiktenko, A. Fedorov, O. V. Man'ko, and V. I. Man'ko, *Phys. Rev. A*, **91**, 042312 (2015).
13. E. Kiktenko, A. Fedorov, A. Strakhov, and V. I. Man'ko, *Phys. Lett. A*, **379**, 1409 (2015).
14. M. A. Man'ko and V. I. Man'ko, *Phys. Scr.*, **T160**, 014030 (2014).
15. V. I. Man'ko and L. Markovich, *J. Russ. Laser Res.*, **35**, 518 (2014).
16. V. N. Chernega and O. V. Man'ko, *J. Russ. Laser Res.*, **35**, 27 (2014).
17. V. N. Chernega, O. V. Man'ko, and V. I. Man'ko, arXiv:1412.6771 quant-ph (2014); *Found. Phys.*, doi : 10.1007/s10701-015-9890-9 (2015).

18. M. A. Man'ko and V. I. Man'ko, *Int. J. Quantum Inform.*, **12**, 156006 (2014).
19. V. N. Chernega and O. V. Man'ko, arXiv:1504.03858, *Phys. Scr.*, **90**, 074052 (2015).
20. Y. P. Shalibo, "Control and measurement of multilevel states in the Josephson phase circuit," PhD Thesis, Hebrew University of Jerusalem (2012).
21. N. Katz and Y. Shalibo, private communication.
22. B. D. Josephson, *Phys. Lett.*, **1**, 251 (1962).
23. J. M. Martinis, S. Nam, J. Aumentado, and C. Urbina, *Phys. Rev. Lett.*, **89**, 117901 (2002).
24. M. Neeley, M. Ansmann, R. C. Bialczak, et al., *Science*, **325**, 722 (2009).
25. M. A. Man'ko and V. I. Man'ko, *Entropy*, **17**, 2876 (2015).
26. J. von Neumann, *Mathematical Foundations of Quantum Mechanics*, Princeton University Press (1955), Vol. 2.
27. E. H. Lieb and M. B. Ruskai, *Inequalities*, Springer (2002), p. 63.